UNIVERSITY OF BIRMINGHAM
University of Birmingham Research at Birmingham

Dynamic functional connectivity following cochlear implantation

Esmaelpoor, Jamal; Peng, Tommy; Jelfs, Beth; Mao, Darren; Shader, Maureen J.; McKay, Colette M.

DOI:
10.1073/pnas.2505086122

License:
Creative Commons: Attribution-NonCommercial-NoDerivs (CC BY-NC-ND)

Document Version
Publisher's PDF, also known as Version of record

Citation for published version (Harvard):
Esmaelpoor, J, Peng, T, Jelfs, B, Mao, D, Shader, MJ & McKay, CM 2025, 'Dynamic functional connectivity following cochlear implantation: Predicting speech outcomes and exploring brain network dynamics', *Proceedings of the National Academy of Sciences of the United States of America*, vol. 122, no. 51, e2505086122. https://doi.org/10.1073/pnas.2505086122

Link to publication on Research at Birmingham portal

General rights
Unless a licence is specified above, all rights (including copyright and moral rights) in this document are retained by the authors and/or the copyright holders. The express permission of the copyright holder must be obtained for any use of this material other than for purposes permitted by law.

•Users may freely distribute the URL that is used to identify this publication.
•Users may download and/or print one copy of the publication from the University of Birmingham research portal for the purpose of private study or non-commercial research.
•User may use extracts from the document in line with the concept of 'fair dealing' under the Copyright, Designs and Patents Act 1988 (?)
•Users may not further distribute the material nor use it for the purposes of commercial gain.

Where a licence is displayed above, please note the terms and conditions of the licence govern your use of this document.

When citing, please reference the published version.

Take down policy
While the University of Birmingham exercises care and attention in making items available there are rare occasions when an item has been uploaded in error or has been deemed to be commercially or otherwise sensitive.

If you believe that this is the case for this document, please contact UBIRA@lists.bham.ac.uk providing details and we will remove access to the work immediately and investigate.

Download date: 08. Nov. 2026

PNAS RESEARCH ARTICLE | PSYCHOLOGICAL AND COGNITIVE SCIENCES

Dynamic functional connectivity following cochlear implantation: Predicting speech outcomes and exploring brain network dynamics

Jamal Esmaelpoor[a,b,1], Tommy Peng[a,b], Beth Jelfs[c], Darren Mao[a,b], Maureen J. Shader[d], and Colette M. McKay[a,b]

Affiliations are included on p. 9.

Edited by Andrew J. Oxenham, Regents of the University of Minnesota, Minneapolis, MN; received March 4, 2025; accepted November 11, 2025 by Editorial Board Member J. Anthony Movshon

Cochlear implants (CIs) have transformed hearing restoration for individuals with severe or profound hearing loss, yet outcomes vary widely and remain difficult to predict. This study introduces an approach by examining the temporal dynamics of brain functional networks postimplantation to identify predictors of outcomes and explore brain plasticity. Twenty-nine CI candidates and 23 normal-hearing individuals participated. Functional near-infrared spectroscopy measured brain activity during audio-only and visual-only speech tasks at 1 mo and 1 y postimplantation, with speech understanding assessed after 1 y. Brain community dynamics were analyzed using multilayer modularity and network switching rates to capture temporal reorganization. Lower network switching rates shortly after implantation were associated with better long-term speech performance. Evidence of cross-modal plasticity—reflecting preimplant neural reorganization—was observed in early recordings, indicated by increased module allegiance between the posterior temporal (PT) region and visual cortices, which diminished after 1 y. Additionally, interhemispheric connectivity in the PT showed significant improvement between sessions, reducing disparities between CI users and normal-hearing individuals. These findings highlight dynamic functional connectivity as a meaningful neural correlate of outcome variability, with potential relevance for guiding personalized rehabilitation strategies and optimizing auditory and speech outcomes.

cochlear implant | outcome prediction | fNIRS | dynamic functional network | brain plasticity

Significance

A substantial proportion of cochlear implant (CI) users—nearly 30%—derive limited benefit from the device, and the neural factors underlying this variability remain poorly understood. This study introduces an approach by analyzing the brain's dynamic community structure using fNIRS, a noninvasive imaging tool compatible with CIs. We show that the stability of brain network organization shortly after implantation predicts future speech understanding. In addition, we demonstrate how brain regions reorganize over time, including reductions in cross-modal plasticity and improvements in interhemispheric connectivity. These findings reveal that dynamic brain metrics offer meaningful insights into individual recovery trajectories and could guide personalized rehabilitation strategies.

Cochlear implants (CIs), widely regarded as one of the most successful neural prostheses, are designed to restore hearing in individuals with severe to profound hearing loss. While CIs have substantially improved functional hearing for many deaf individuals, approximately 30% of users derive limited benefit or struggle to use the device effectively (1). Despite extensive research, case-history factors—such as duration of deafness, age of hearing loss, residual hearing, and prior hearing aid experience—explain less than 20% of the variability in implantation outcomes (2–4). This limited predictive power has shifted the research focus toward identifying more robust predictors of speech understanding outcomes. Our study is investigating the role of the central language networks as the ultimate processing centers for auditory and speech-related information in the recovery of speech understanding after CI. Identifying brain-related features linked to CI outcomes could enable subject-specific adjustments to CI devices and the development of more targeted rehabilitation therapies.

Numerous studies have investigated cross-modal and intermodal brain activations in response to different auditory and visual tasks, revealing neuroplastic changes following hearing loss and cochlear implantation (5–12). These neuroplastic changes have been associated with variations in speech understanding outcomes. Similarly, studies on brain functional networks—both under resting-state and task-based conditions—have provided insights into neural plasticity and identified potential biomarkers for speech performance (13–16). However, most of this work has focused on static network properties, overlooking the temporal dynamics of brain functional networks. This study investigates the dynamic community structure of brain functional networks in the context of cochlear implantation, with the aim of identifying indicators of speech outcomes and examining neural plasticity following implantation.

In this study, we examine the temporal dynamics of brain functional networks following cochlear implantation. Brain functional networks are organized into *modular structures*—clusters of regions that are densely connected within themselves but more sparsely connected to other modules. This modular organization supports functional

Author contributions: J.E., T.P., B.J., D.M., M.J.S., and C.M.M. designed research; J.E. performed research; J.E. contributed new reagents/analytic tools; J.E. analyzed data; T.P., B.J., D.M., M.J.S., and C.M.M. reviewed and edited the manuscript; and J.E. wrote the paper.

The authors declare no competing interest.

This article is a PNAS Direct Submission. A.J.O. is a guest editor invited by the Editorial Board.

Copyright © 2025 the Author(s). Published by PNAS. This article is distributed under Creative Commons Attribution-NonCommercial-NoDerivatives License 4.0 (CC BY-NC-ND).

[1]To whom correspondence may be addressed. Email: jesmaelpoor@bionicsinstitute.org.

This article contains supporting information online at https://www.pnas.org/lookup/suppl/doi:10.1073/pnas.2505086122/-/DCSupplemental.

Published December 15, 2025.

Downloaded from https://www.pnas.org by UNIVERSITY OF BIRMINGHAM on January 16, 2026 from IP address 147.188.245.153.

segregation, allowing specialized processing within distinct subnetworks. However, these modular patterns are not static; they dynamically reconfigure over time to meet changing cognitive demands (17). To capture this reorganization, we track the evolving community structure of the brain using a multilayer network model and compute the *network switching rate*[*], which quantifies how frequently each region transitions between different functional communities. Higher switching rates reflect greater instability or flexibility in modular affiliation over time (18). Previous research has demonstrated the relevance of brain temporal dynamics in understanding cognitive processes and learning (17–19). Building on these studies, we hypothesize that CI users' brain dynamics influence speech understanding. By analyzing these temporal brain network dynamics, we aim to identify key features that explain variability in CI users' speech understanding performance after 1 y of implantation and offer insights into brain plasticity during hearing restoration.

The brain functions as a highly complex and interconnected system that continuously adapts to environmental demands across a wide range of temporal scales, from milliseconds to years (20). This adaptability is governed by two core principles: temporal dynamics and interconnectivity. Brain regions and their associated networks engage in tasks differently depending on both the timing and nature of the task, exhibiting either transient or sustained activations. Therefore, a comprehensive understanding of cognitive processes, such as speech understanding, requires consideration of the brain's dynamic and interconnected nature (17, 21).

Brain adaptability is further supported by cortical modularity, which refers to the organization of brain networks into distinct yet interdependent subsystems, or "modules." These modules perform specialized functions with minimal disruption to the overall network. Importantly, brain modularity is hierarchically organized, with meaningful community structures observed at multiple spatial scales, from fine-grained local circuits to broader functional systems (22). The brain's modular organization is also dynamic, requiring flexibility to adapt existing networks and precision to engage new processes for specific tasks. This dynamic modular architecture is critical for brain evolution, development, and optimal cognitive functioning (21).

In this study, we employed functional near-infrared spectroscopy (fNIRS), a noninvasive and cost-effective brain imaging technique that measures cortical activity by detecting changes in blood oxygenation and volume (23). Notably, fNIRS is fully compatible with CIs, enabling us to examine cortical activity without electrical interference from the device (24). To evaluate brain dynamics, we constructed functional brain networks for successive time intervals during a task-based experiment involving auditory and visual speech tasks (Figs. 1 and 2). This method allowed us to create a multilayer network that integrates both spatial and temporal connectivity across brain regions. To analyze the evolving brain community structure over time, we used the multilayer modularity algorithm proposed by Mucha et al. (25). This algorithm decomposes the multilayer network into spatiotemporal modules, estimating the dynamic segregation of brain regions into subsets of nonoverlapping communities across time and space. To quantify changes within these modular structures, we calculated network switching rate (17, 18). We hypothesized that network switching during the experiment correlates with CI users' speech understanding abilities, serving as a dynamic brain network metric to explain variability in performance.

[*]Network switching is also called flexibility in some studies.

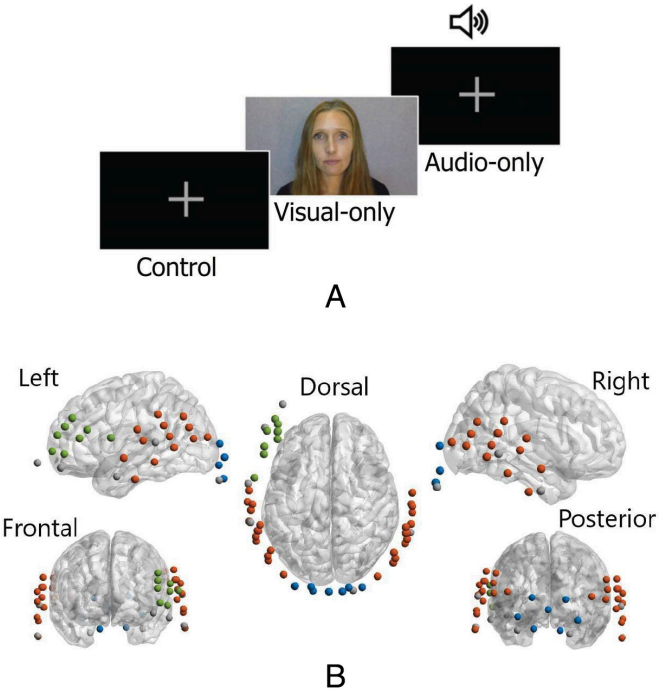


Fig. 1. Experimental design and fNIRS montage. (*A*) Participants were presented with 36 contextually connected segments from a children's story, including 18 audio-only and 18 visual-only trials, along with 10 control trials featuring a gray fixation cross. (*B*) The fNIRS montage included 44 long channels and eight short channels. Coverage areas included the inferior frontal gyrus (green), bilateral auditory cortices (red), and occipital lobe (blue). Short channels, used to capture systemic artifacts, are shown in gray.

Furthermore, we investigated two critical aspects of brain plasticity following hearing loss and cochlear implantation: cross-modal connectivity and interhemispheric auditory connectivity. Specifically, we assessed changes in module allegiance between pairs of regions in auditory and visual areas to evaluate cross-modal plasticity, and between auditory regions across hemispheres to examine interhemispheric interactions. In contrast to switching rate, which captures how often a single region changes its module affiliation over time, module allegiance quantifies the probability that pairs of regions are assigned to the same community across time windows. Higher allegiance indicates more consistent functional integration between two regions, making this metric particularly suitable for examining cross-system and interhemispheric reorganization. By analyzing these processes from a dynamic brain network perspective, our study provides insights that complement existing literature focused primarily on regional activation, static connectivity, or structural organization—thus advancing our understanding of neural reorganization following cochlear implantation.

Results

To assess the dynamics of brain functional connectivity following cochlear implantation, we conducted a task-based fNIRS experiment involving audio-only and visual-only speech tasks (Fig. 1*A*). The optode montage captured activity across bilateral auditory cortices, inferior frontal areas, and the occipital lobe using long and short channels (Fig. 1*B*). To characterize temporal changes in brain network organization, we applied a dynamic community detection approach proposed by Mucha et al. (25) (Fig. 2 *A*–*C*) and extracted three key features—network switching, module allegiance, and community similarity (Fig. 2 *D* and *E*)—which are described in detail in the Methods section.

Downloaded from https://www.pnas.org by UNIVERSITY OF BIRMINGHAM on January 16, 2026 from IP address 147.188.245.153.

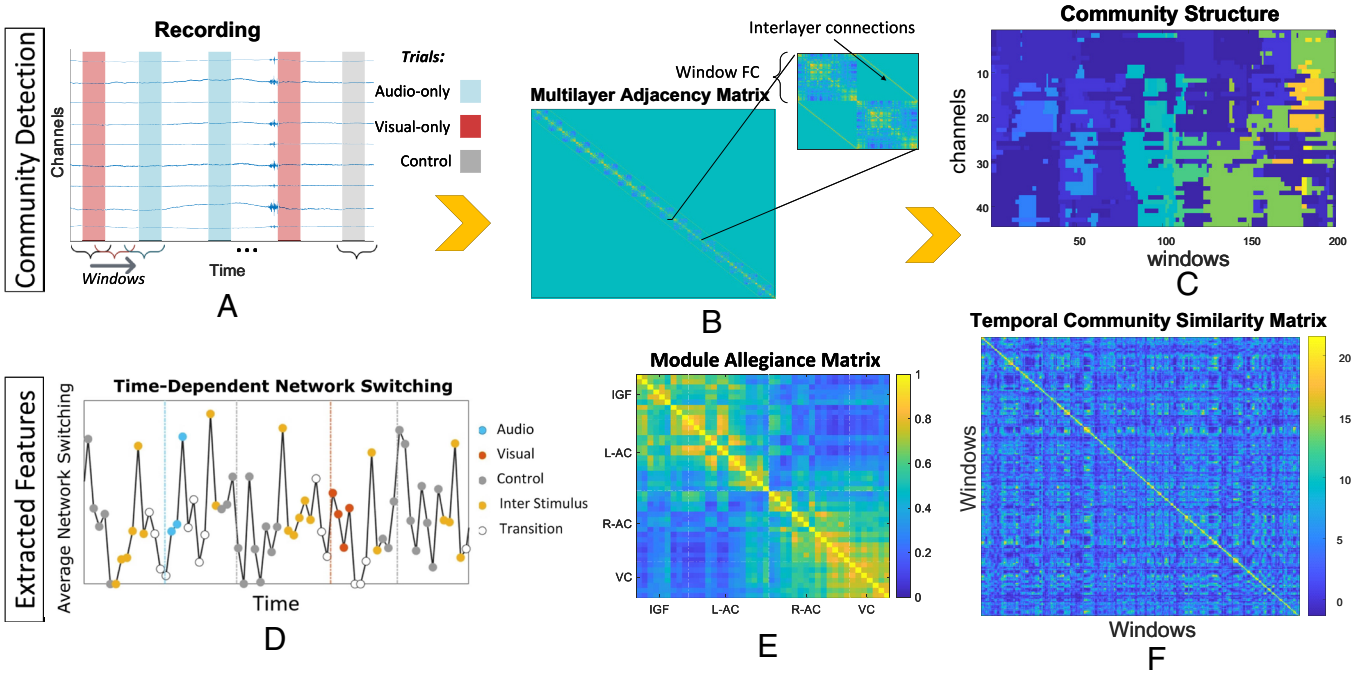


Fig. 2. Community detection pipeline: (*A*) A sliding-window Pearson's correlation approach was applied to estimate functional connectivity between all pairs of fNIRS channels within each time window. (*B*) Layer-specific adjacency matrices were combined into a single multilayer adjacency matrix, with interlayer connections coupling each node with itself across adjacent layers. (*C*) Community detection was performed using a multilayer adaptation of the Louvain modularity-optimization algorithm, partitioning the network into nonoverlapping communities across time. Extracted Features: (*D*) *Time-dependent network switching* quantifies how frequently each brain region switches its modular allegiance over time, normalized by the total number of possible changes. (*E*) *Module allegiance matrix* captures the probability that any two brain regions (nodes) are part of the same module throughout the experiment. (*F*) *Temporal community similarity matrix* measures the similarity of brain community structures across different time steps.

Higher Network Switching Rates 1 mo Postimplant Predict Poorer Speech Understanding at 12 mo. A key objective of this study was to explore brain dynamics and identify potential predictors of cochlear implantation outcomes, with a focus on the dynamic properties of brain community structures. To this end, we examined the relationship between average network switching across all nodes in fNIRS recordings taken 1 mo after switch-on and speech performance outcomes, assessing its predictive value for implantation success. Our findings revealed a significant negative correlation ($P < 0.05$) between network switching measured at the first fNIRS recording and speech performance outcomes at 12 mo postimplantation. Fig. 3*A* illustrates these correlations for two speech tests—CNC phonemes in quiet and BKB sentences in noise—at the first recording session. We also assessed the correlation between network switching at the second recording session, conducted 1 y postimplantation, and speech scores; however, these associations were no longer statistically significant (*SI Appendix*). We clarify that the second recording was not intended for outcome prediction, as it coincides with the time of outcome assessment, and was instead used to evaluate brain plasticity.

Interstimulus Network Switching Primarily Drives the Correlation between Network Switching 1 mo Postimplantation and Speech Outcomes. To further investigate the relationship between network switching in the first fNIRS recording (1 mo postimplantation) and speech performance outcomes, we conducted exploratory analyses to assess the correlation between network switching during specific experimental conditions—auditory, visual, control trials, and interstimulus intervals (ISI)—and speech outcomes. Our analysis revealed that the significant correlation between network switching in the first fNIRS session and speech performance at 12 mo postimplantation was primarily driven by the strong association between network switching in the ISI condition and speech outcomes. Fig. 3*B* illustrates these correlations, highlighting the relationship between ISI-related network switching during the first fNIRS recording and speech performance. In contrast, as detailed in the *SI Appendix*, section S4, network switching during trial conditions (auditory, visual, and control trials) did not show significant correlations with speech outcomes. *P*-values were adjusted using the Benjamini–Hochberg method to account for multiple comparisons and control the false discovery rate.

To confirm the robustness of this association, we included age, deafness duration, and hearing threshold in the nonimplant ear in multivariable models. Network switching during ISI remained a significant predictor of speech outcomes, while none of the clinical variables reached significance (*SI Appendix*).

Dynamic Brain Community Structures are More Stable in NH Subjects Compared to CI Users. To further investigate the evolution of brain network stability over the course of the experiment, we analyzed the temporal stability of community structures using fNIRS recordings from NH subjects and from the first and second recording sessions of CI users. Stability was quantified using the temporal community similarity matrix, which assesses the similarity of community structures between pairs of windows, measured using z-Rand scores (26). Similarity values were averaged over different numbers of adjacent windows (ranging from 2 to 15; *SI Appendix*), and time-domain similarity curves were generated for each set of recordings. Fig. 4*A* illustrates the smoothed average similarity curve for two successive windows (n = 2), with shaded areas indicating the SEM. Additional curves for other window sizes are provided in the *SI Appendix*.

Downloaded from https://www.pnas.org by UNIVERSITY OF BIRMINGHAM on January 16, 2026 from IP address 147.188.245.153.

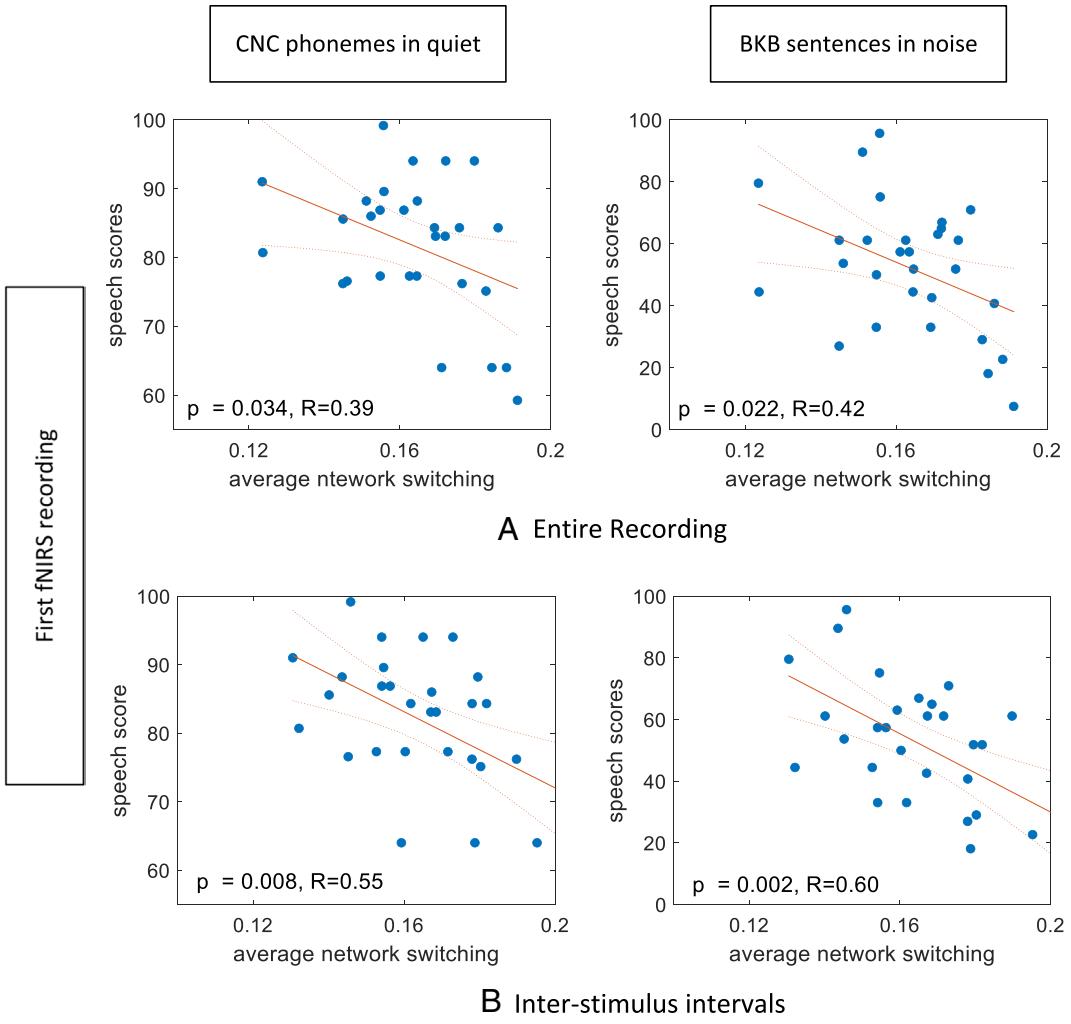


Fig. 3. Correlations between network switching and speech performance. (*A*) Correlation between average network switching and speech scores for CNC phonemes in quiet and BKB sentences in noise across the full recording session, 1 mo postimplantation. (*B*) Correlations during interstimulus intervals (ISI), highlighting a stronger relationship between switching rates and speech performance in these periods.

The figure reveals that the similarity curve for NH subjects consistently remained higher than those for CI users at both recordings. To statistically validate these observations, we employed a linear mixed-effects (LME) model to evaluate the effects of group and time on community similarity, while accounting for random intercepts for subjects and temporal variability: Community Similarity ~ Group + Time + (1 + Time|Subject). Across all values of n (n ranging from 2 to 15), the results consistently showed that both CI recording sessions exhibited significantly lower community similarity compared to the NH group ($\Delta \approx -0.8$, $P < 0.001$), with no significant difference between CI users 1 mo and 1 y postimplantation. The fitted LME curves are plotted in Fig. 4*B* to highlight these results.

Next, we examined the effect of time on community similarity curves during the experiment for each recording set individually. A linear mixed-effects model was used for each group of recordings, incorporating time as a fixed effect and subject as a random effect: Community Similarity ~ Time + (1|Subject). The results showed no significant change in community similarity over time for NH subjects or for CI users 1 y postimplantation. However, a significant reduction in community similarity over time was observed for CI users 1 mo postactivation ($P < 0.001$), indicating time-dependent changes in the community structure for this recording set.

As introduced in the Methods section, network switching quantifies how frequently nodes change their community assignments and serves as an indicator of instability in the community structure—complementary to the stability captured by community similarity. Based on the observed differences in community similarity, we further compared the time-dependent average network switching across groups. Notably, the findings were consistent with those from community similarity, exhibiting the expected inverse trend. Supporting this relationship, *SI Appendix*, Fig. S9 shows a strong negative correlation (R > 0.90) between time-dependent network switching rates and community similarity for two successive windows.

Fig. 4*C* illustrates the time-dependent network switching curves for subjects in all recording sets, showing that NH recordings exhibited lower network switching compared to CI user recordings at both time points, reflecting greater stability in the NH group. Statistical analysis using a similar mixed-effects model used for comparing community similarity revealed that network switching was significantly higher for CI users (both 1 mo postactivation and 1 y postimplantation) compared to NH subjects ($\Delta \approx 0.008$, $P < 0.001$), with no significant difference between the two recordings for CI user. Regarding the effect of time, a significant increase in time-dependent network switching was observed for CI users 1 mo postactivation ($P < 0.001$), indicating temporal changes in

Downloaded from https://www.pnas.org by UNIVERSITY OF BIRMINGHAM on January 16, 2026 from IP address 147.188.245.153.

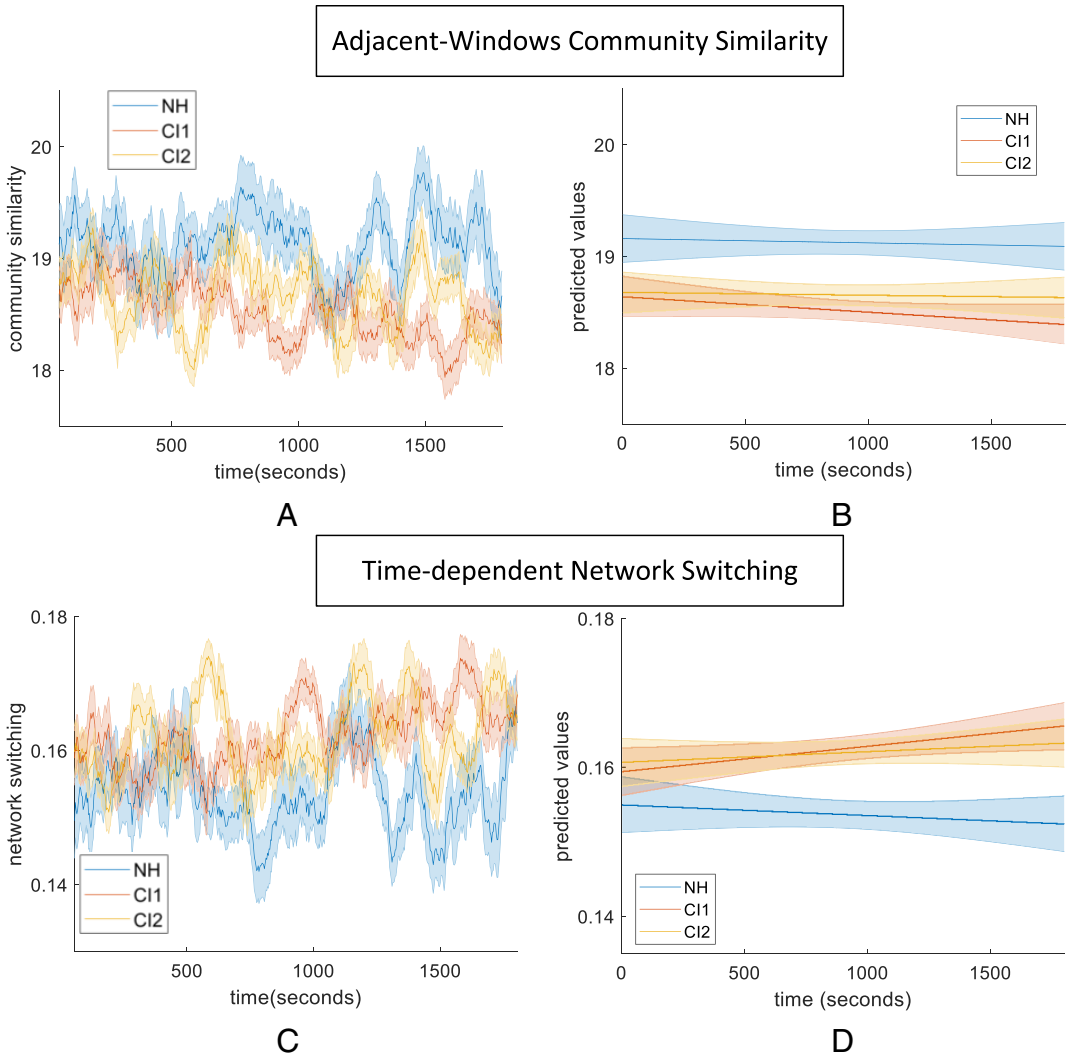


Fig. 4. Community similarity and network switching across groups of recordings. (*A*) Average community similarity curves for two adjacent windows (n = 2), with shaded areas showing SEM. (*B*) Linear mixed-effects model (LME) fit curves for community similarity. (*C*) Average time-dependent network switching curves for all groups, with shaded areas representing SE. (*D*) LME fit curves for time-dependent network switching. All curves were smoothed using a sliding window averaging over 30 samples to enhance visual comparison of amplitude and trends.

community dynamics. Conversely, no significant changes over time were observed for NH subjects or for CI users 1 y postimplantation. The fitted LME curves are included in Fig. 4*D* to highlight these results.

These findings demonstrate a consistent relationship between the two measures—community similarity and time-dependent network switching—highlighting that NH subjects exhibit more stable brain community structures, whereas CI users show greater instability.

Cross-Modal Plasticity Revealed by the Allegiance Matrix Following Cochlear Implantation. Loss of a sensory modality, such as hearing in cases of postlingual hearing loss, induces cross-modal plasticity in the brain. In response, remaining modalities, such as vision, engage with auditory areas, leading to a partial repurposing of cortical regions previously dedicated to the lost modality (27).

To examine cross-modal plasticity through dynamic functional connectivity, we analyzed the average module allegiance between channels in the visual cortex and two restricted temporal regions: the posterior temporal (PT) region, encompassing the angular gyrus, and the mid-temporal (MT) region, spanning portions of the superior and middle temporal gyri, as described by Shader et al. (24). Cross-modal interaction, quantified through the module allegiance metric, measures the probability that nodes from the visual cortex and either MT or PT belong to the same module.

We assessed two key aspects of cross-modal plasticity: 1) whether deafness led to increased audio-visual allegiance in CI users (first session) compared to NH individuals, and 2) whether this allegiance changed with CI experience. As shown in Fig. 5, our analysis revealed no significant differences in the average cross-modal allegiance involving PT across different recording sets. In contrast, MT exhibited significantly higher cross-modal allegiance in CI users 1 mo after device activation compared to NH individuals. However, this difference was no longer significant 1 y postimplantation, suggesting a trend toward adaptive plasticity in auditory regions between the first and second recordings. The early cross-modal activity likely reflects the effects of long-term auditory deprivation, as functional brain reorganization following cochlear implantation is known to require several months to emerge (14, 28).

Additionally, we compared the average cross-modal allegiance between PT and MT across different recordings. The results

Downloaded from https://www.pnas.org by UNIVERSITY OF BIRMINGHAM on January 16, 2026 from IP address 147.188.245.153.

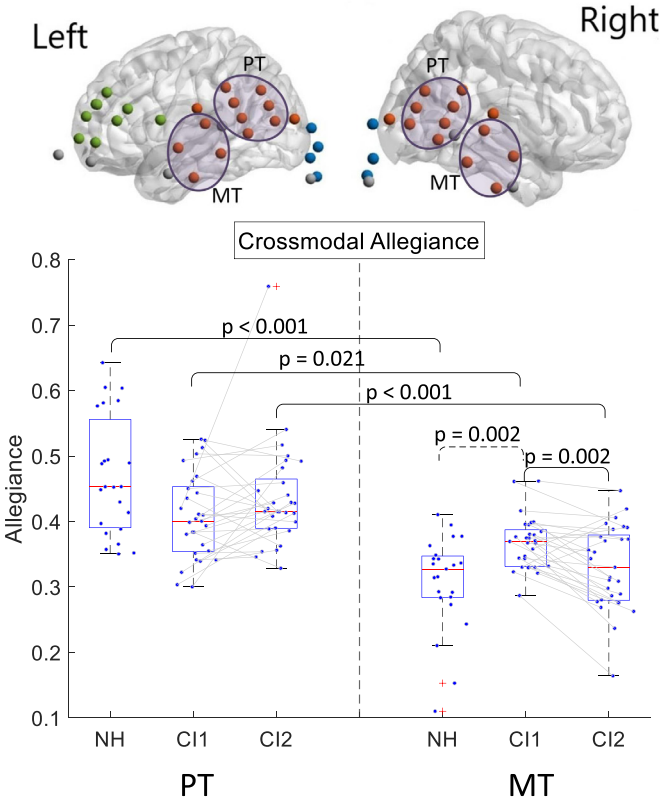


Fig. 5. Cross-modal interaction between visual and auditory regions. Average module allegiance between nodes in the visual cortex and auditory regions within the PT and MT across different recording sessions. Cross-modal interaction was quantified using the module allegiance metric.

indicated that module allegiance between the visual cortex and MT was significantly lower than that between the visual cortex and PT. This finding suggests that PT, being topologically closer to the visual cortex, exhibits stronger functional collaboration with visual areas than MT during auditory and visual speech tasks.

P-values were adjusted using the Benjamini–Hochberg method to account for multiple comparisons and control the false discovery rate.

Interhemispheric Plasticity Revealed by the Allegiance Matrix Following Cochlear Implantation. Hearing loss is known to induce both structural and functional alterations in interhemispheric connectivity between auditory cortices, which can significantly impact auditory processing (29–33). Building on this knowledge, we investigated interhemispheric plasticity following cochlear implantation, comparing CI users to NH participants from a dynamic functional connectivity perspective using the allegiance matrix. To achieve this, we focused on two specific auditory regions within the montage: MT and PT. Interhemispheric cooperation between these regions in opposing hemispheres was quantified using the allegiance matrix and compared across different recording sets (Fig. 6). Our findings indicate no significant differences in average interhemispheric allegiance for pairs of nodes within the PT across recording sets. However, average interhemispheric allegiance between channels in MT regions showed notable improvements 1 y after implant activation. This enhancement in allegiance reduced the initial gap observed between NH participants and CI users during the first recording session. As a result, by the second session, the difference in MT interhemispheric allegiance between NH and CI users was no longer significant, suggesting adaptive plasticity in auditory regions over time, as observed in longitudinal changes between the first and second recordings following cochlear implant use. P-values were adjusted using the Benjamini–Hochberg method to account for multiple comparisons and control the false discovery rate.

Discussion

Advancing Cochlear Implant Research through Dynamic Functional Connectivity Analysis. In this study, we explored the dynamics of brain functional connectivity in a task-based experiment involving audio-only and visual-only speech tasks, using fNIRS to identify reliable indicators of cochlear implantation outcomes and examine key aspects of brain plasticity following implantation. Previous research on predicting speech performance outcomes for CI users and brain plasticity after implantation based on brain imaging data can be broadly classified into two main approaches. The first focuses on assessing regional brain activation patterns in response to visual or audio stimuli. The second examines static functional connectivity networks during resting or task-based conditions. Our approach extends these conventional methodologies by evaluating the temporal dynamics of brain functional networks, specifically focusing on the evolution of brain community structures over time. This perspective complements static brain network analyses by capturing temporal variations in functional connectivity metrics, offering deeper insights into the fundamental properties of brain networks (17, 34). Additionally, techniques assessing regional brain activation inherently measure fluctuations in the hemodynamic response to tasks, reflecting changes in amplitude over time. These methods can be considered as evaluating the dynamics of regional hemodynamic responses, making them a counterpart to the dynamic functional connectivity techniques employed in our study, which focus on the evolving interactions within brain networks. Notably, these

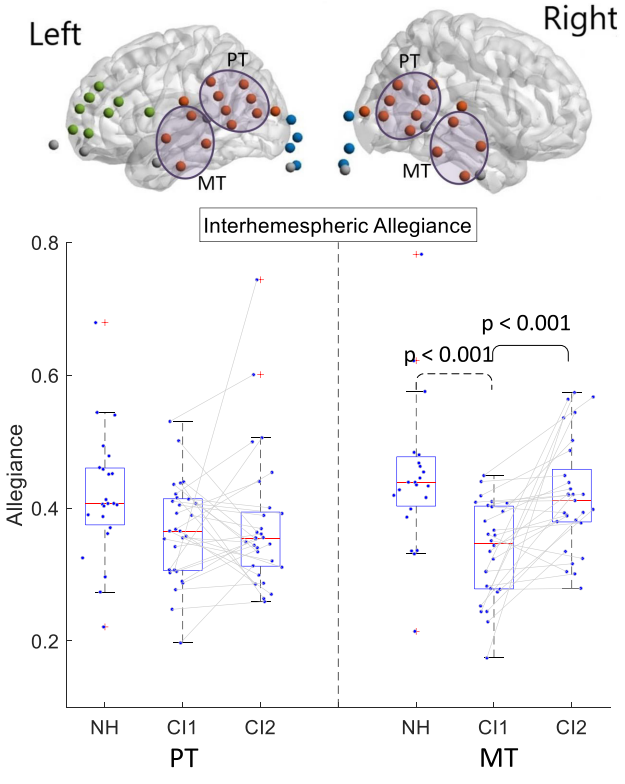


Fig. 6. Interhemispheric interaction in auditory regions. Average module allegiance between bilateral auditory regions within the PT and MT groups. Interhemispheric interaction was assessed using the module allegiance metric.

Downloaded from https://www.pnas.org by UNIVERSITY OF BIRMINGHAM on January 16, 2026 from IP address 147.188.245.153.

two approaches reflect distinct but interconnected principles of brain organization. Regional brain activation studies emphasize the segregation principle, focusing on localized, task-specific activity. In contrast, dynamic functional connectivity approaches align with the integration principle, examining how distributed brain regions interact and reorganize over time to support complex cognitive functions (35).

Predicting Cochlear Implant Outcomes through Network Switching Dynamics. Dynamic changes in the brain's functional modular (community) structure during the experiment session were quantified using network switching, which measures how frequently brain regions change their modular allegiance. Our analysis revealed a significant negative correlation between the switching rate measured during the first recording, 1 mo postimplantation, and speech outcomes measured 1 y later (Fig. 3*A*). Notably, this correlation was primarily driven by ISI condition, where lower network switching rates predicted better speech performance (Fig. 3*B*). The ISI intervals should not be interpreted as baseline resting state. Instead, they represent transient periods in which brain networks return toward baseline after task-related perturbations. Our prior fNIRS studies (15, 36) have shown that ISIs more closely resemble task-related activity than pre-experiment resting-state scans, suggesting that ISIs capture important transitional dynamics between task conditions. This may explain why network reconfiguration during ISIs, rather than during active task blocks, provided the most informative link to speech outcomes. These results suggest that CI users whose brain networks exhibited greater stability (lower switching rate) during ISI intervals shortly after implantation achieved better long-term outcomes. Comparisons between NH participants and CI users also demonstrated that NH individuals exhibited greater stability in their functional modular structures (Fig. 4).

Dynamic reconfiguration of brain networks often occurs in response to changing cognitive demands or environmental stimuli, involving the activation or inhibition of specific neural pathways, the reallocation of neural resources, and increased communication between regions—all of which are metabolically expensive (34, 37, 38). In this study, lower network switching in the ISI condition 1 mo postimplantation predicted better speech understanding at 12 mo. This suggests that reduced poststimulus reorganization early after implantation may reflect a more stable neural network configuration, which could be beneficial for long-term adaptation to auditory input. Alternatively, greater switching may indicate increased preimplant plasticity, which could reflect ongoing compensatory processes that do not necessarily translate into better speech outcomes.

Restoration of Auditory Function and Cross-Modal Adaptation in CI Users. The introduction of auditory stimulation post-CI triggers plasticity in visual and auditory cortices, enabling the brain to adapt to the novel stimuli. As shown in Fig. 5, our results evaluating average module allegiance for pairs of nodes in the visual cortex and restricted auditory areas of PT and MT indicate that CI users shortly after implantation demonstrated stronger cross-modal integration of the auditory cortex and visual cortex specifically in MT compared to NH controls. This difference diminished after 1 y of using the device indicating that MT retrieves its auditory functionality due to the hearing stimuli provided by the device. Additionally, consistent with the brain's economy principle, average cross-modal allegiance with PT—given its closer anatomical proximity to the visual cortex—was consistently higher than with MT across all recording sets. This observation aligns with the concept of topological efficiency, wherein neural elements and their connections are spatially constrained, making material and metabolic costs critical considerations in brain network organization (39, 40).

Improved Interhemispheric Cooperation in Auditory Cortices Following CI Use. We assessed another critical aspect of brain plasticity: interhemispheric connectivity. As shown in Fig. 6, our findings reveal that interhemispheric allegiance improves significantly after 1 y of cochlear implant use. Moreover, the initial differences observed between NH individuals and CI recipients in interhemispheric connections within MT 1 mo postimplantation diminish by the second recording 1 y after implantation.

Previous studies indicate that hearing loss significantly disrupts interhemispheric connectivity between auditory cortices, causing functional and structural alterations in auditory pathways. In the absence of normal auditory input, auditory cortices often undergo cross-modal plasticity, becoming responsive to other sensory modalities, such as vision or touch, which disrupts typical connectivity across hemispheres (41). Moreover, the corpus callosum, particularly its posterior portion that connects the left and right auditory cortices, plays a critical role in mediating interhemispheric interactions. Hearing loss can alter these pathways, hindering the efficient transfer of auditory information between hemispheres (29, 30, 42). This disruption likely explains the initial differences in interhemispheric connectivity observed between NH individuals and CI recipients 1 mo postimplantation in our study, reflecting the impact of prolonged auditory deprivation on neural pathways.

Our findings demonstrate improved interhemispheric integration over the first year of CI cochlear implantation. Enhanced collaboration of MT nodes across hemispheres within the same functional module supports the idea that hearing aids or cochlear implants promote neuroplasticity. This intervention restores interhemispheric connectivity, reduces asymmetries associated with hearing loss, and fosters auditory information integration. Such interhemispheric cooperation is essential for supporting language-related tasks and spatial hearing (43, 44).

Conclusion

This study introduces an approach to investigating dynamic brain functional networks following cochlear implantation, emphasizing the role of temporal network reorganization in predicting outcomes. We identified network switching rates as an early indicator of speech understanding, with more stable networks—similar to those of normal-hearing individuals—linked to better outcomes. Improvements in interhemispheric connectivity within the mid-temporal and reduced cross-modal reorganization over time likely reflect the brain's adaptive recovery of auditory function, with early cross-modal activity representing the effects of prolonged auditory deprivation. These findings highlight the value of dynamic connectivity metrics in capturing brain flexibility and suggest their relevance for understanding individual differences in neural adaptation, which may inform future approaches to personalized rehabilitation in cochlear implant users.

Materials and Methods

Participants. This study included thirty-one English-speaking adult CI recipients who were postlingually deafened and had recently undergone cochlear implantation. No additional recruitment criteria were applied. However, data from two participants were excluded: one due to missing speech performance scores and another due to poor data quality. Consequently, analyses were performed on twenty-nine CI recipients (mean age: 59.6 ± 14 y; 17 males, 12 females; see

Downloaded from https://www.pnas.org by UNIVERSITY OF BIRMINGHAM on January 16, 2026 from IP address 147.188.245.153.

demographic details in *SI Appendix*, Table S1). A control group of twenty-three age-matched individuals with normal hearing (NH) considering their age also participated (mean age: 62.0 ± 14 y; 11 males, 12 females). Hearing thresholds for the NH group were assessed, with pure-tone averages (PTA) confirmed to be below 30 dBHL in both ears. Ethics approval was granted by the Royal Victorian Eye and Ear Hospital Human Research Ethics Committee (ethics approval no. 19.1418H), and all participants provided written informed consent prior to participation.

To ensure that cognitive decline did not influence the study outcomes, cognitive functioning was assessed for all CI users using the Trail Making Test parts A and B (45). In part A, participants were instructed to connect numbers sequentially in ascending order as quickly as possible, while part B required alternating connections between numbers and letters in ascending order. Both tasks were completed on paper, with the items randomly arranged. Participants were asked to perform the tasks efficiently and without lifting the pencil from the paper. Performance for all participants was within the normal range, based on age- and education-adjusted norms as defined by (46).

Speech performance outcomes for CI users were evaluated 1 y following device activation. Two audio-only speech tests were conducted to measure their speech understanding abilities. The first test consisted of 50 consonant–nucleus–consonant (CNC) words presented in quiet (47). The second test featured 15 Bamford-Kowal-Bench (BKB) sentences delivered in four-talker babble noise at a signal-to-noise ratio (SNR) of 10 dB (48). Speech stimuli were presented at a comfortable listening level of 65 dBA through free-field speakers. To ensure performance reflected CI use, the contralateral ear was masked or occluded as needed. Performance on the CNC test was quantified as the percentage of correct phonemes identified, while scores for the BKB sentences were expressed as the percentage of correctly repeated words. Speech scores were subsequently transformed into rationalized arcsine units for statistical analysis (49).

Experiment. The study employed a task-based experimental design featuring both audio-only and visual-only speech tasks, as described by Shader et al. (24). Participants were comfortably seated in a sound-attenuated booth, facing a monitor screen, with a loudspeaker placed one meter away for auditory stimulus delivery at 55 dBA in free-field conditions. The experimental procedure (Fig. 1*A*) involved the presentation of 36 contextually connected segments from the children's story Mrs. Tittlemouse by Beatrix Potter, narrated by a female native speaker of Australian English. These story segments were presented in 18 audio-only trials and 18 visual-only trials. Additionally, 10 control trials were included, during which participants attended to a gray fixation cross on the screen with no auditory or visual speech stimuli. Each segment lasted an average of 12.5 s. Intertrial intervals lasting 15 to 30 s followed each segment, during which participants fixated on a gray cross displayed on the screen in silence. To prevent order effects, the segments were pseudorandomized across conditions while maintaining the contextual continuity of the story during the audio and visual trials.

fNIRS Recording. Two fNIRS recording sessions were carried out to examine cortical activity: The first session took place within the first month after implant activation, and the second occurred approximately 1 y postactivation. Both recordings were conducted using the same setup to maintain consistency across sessions. Data acquisition was performed using a continuous-wave NIRScout system (NIRScout, NIRX Medical Technologies, LLC). The montage consisted of 16 sources and 16 photodiode detectors, with each source emitting near-infrared light at dual wavelengths–760 nm and 850 nm. This configuration created 44 long channels with an average source-detector distance of 3 cm. The montage covered the inferior frontal gyrus, the bilateral auditory cortices, and the occipital lobe, as shown in Fig. 1*B*. To minimize contamination from noncortical physiological noise, such as those originating from the scalp, the montage also included eight short channels with a source-detector separation of 8 mm. These short channels were designed to capture extracerebral activity, enabling improved isolation of signals originating from cortical brain regions (23).

Data Preprocessing. Data preprocessing was performed using MATLAB and the NIRS Toolbox (50). The fNIRS recordings were first converted to optical density, and channel quality was assessed using the scalp coupling index (SCI) (51). Channels with SCI values below 0.5 were deemed unreliable and excluded from further analysis. To mitigate motion artifacts, the temporal derivative distribution repair (TDDR) method (52) was applied. The optical density signals were subsequently converted to oxyhemoglobin (HbO) and deoxyhemoglobin (HbR) concentrations using the modified Beer–Lambert law (53). Since long channels capture both cerebral signals and systemic noise–such as heartbeats, respiration, and Mayer waves–additional corrections were applied to isolate neural activity. Short-channel correction involved regressing out the short channel signals, which predominantly capture superficial systemic artifacts, from the long-channel signals (54). A Butterworth band-pass filter (order = 8, range = 0.035 to 0.40 Hz) was then applied to remove residual low-frequency drift and high-frequency cardiac noise. The dynamic connectivity analysis presented here is based on HbO data, as previous studies have demonstrated that HbO yields more robust coherence patterns and connectivity compared to HbR (55). Further details on parameter selection and filtering procedures are provided in the *SI Appendix*.

Dynamic Functional Connectivity and Community Detection. Fig. 2 provides an overview of the processing steps used to evaluate the dynamics of functional connectivity. To analyze the temporal dynamics of brain functional networks, a sliding-window Pearson's correlation approach was employed to estimate functional connectivity between all pairs of fNIRS channels within each time window (Fig. 2*A*). To incorporate temporal dependencies across consecutive windows, we used the multilayer network framework introduced by Mucha et al. (25). In this framework, layer-specific adjacency matrices (each representing functional connectivity within a time window) are combined into a single multilayer adjacency matrix (Fig. 2*B*). Interlayer connections couple each node with itself across adjacent layers, enabling the detection of modular structure while accounting for temporal continuity (20). The multilayer modularity index Q_{ML} is used to optimize the dynamic community structure detection and is formally defined as

$$Q_{ML} = \frac{1}{2\mu} \sum_{ijlr} \left[\left(A_{ijl} - \gamma_l e_{ijl} \right) \delta\left(m_{il}, m_{jl} \right) + \delta_{ij} C_{jlr} \right] \delta\left(m_{il}, m_{jr} \right), \qquad [1]$$

where, A_{ijl} is the sliding-window correlation between nodes i and j at time window l; e_{ijl} represents the Newman–Girvan null model connectivity weight for intramodule connectivity, calculated separately for each layer l (56); γ_l is the topological resolution parameter for layer l, which controls the size of detected communities; C_{jlr} is the temporal coupling parameter for node j between time windows l and r, linking nodes across layers; δ is an indicator function that equals 1 if nodes i and j belong to the same module (m) and 0 otherwise; and μ is the total edge weight in the multilayer network.

The resolution parameter γ influences the granularity of community detection: Larger values favor smaller while smaller values lead to larger modules. The interlayer coupling parameter C determines the temporal persistence of communities across adjacent windows. For the results presented here, we set $\gamma = 1$ and $C = 0.2$. To align with the trial structure and interstimulus intervals in our experiment, we configured the window length to 18 s and the step size between successive windows to 3 s. Additional details on parameter selection are provided in the *SI Appendix*.

We performed community detection using a multilayer adaptation of the Louvain modularity-optimization algorithm proposed by Mucha et al. (25), which partitions the network into disjoint communities across time (Fig. 2*C*). Given the stochastic nature of the algorithm, we repeated the community detection process 50 times for each recording to ensure consistency and reliability in the results.

Feature Extraction. To analyse brain functional dynamics during the experiment, we extracted three features from the detected dynamic community structures.

- Network Switching: Network switching quantifies how frequently each brain region (node) switches its modular allegiance over time, normalized by the total number of possible changes (17). The overall network switching is calculated as the mean network switching across all nodes. We measured network switching both over the entire experiment duration and between consecutive time windows, referring to the latter as *time-dependent* network switching (19). Fig. 2*D* illustrates time-dependent network switching for a sample recording, highlighting its temporal variation. To examine network switching across different conditions, we labeled the sliding window across the entire recording and each timestep based on its overlap with task trials. Specifically, windows that overlapped with at least 90% of a single trial were labeled as *audio*, *visual*, or *control*, depending on the trial type. Windows covering less than 10% of any trial were classified as interstimulus interval (ISI), representing

Downloaded from https://www.pnas.org by UNIVERSITY OF BIRMINGHAM on January 16, 2026 from IP address 147.188.245.153.

periods between task events. Windows spanning between 10% and 90% of one or more trials were considered *transitional* and excluded from analysis to minimize contamination by overlapping cognitive states.

- Module Allegiance Matrix: The module allegiance matrix captures the probability that any two brain regions (nodes) are part of the same module throughout the experiment. Specifically, each element in row j and column i of this symmetric matrix represents the frequency with which nodes j and i share the same module across all time windows, normalized by the total number of windows. Fig. 2*E* illustrates an example of a module allegiance matrix.
- Temporal community similarity matrix: The temporal community similarity matrix (TCS) captures the similarity of brain community structures across different time steps (windows). Each element in row *i* and column *j* of the symmetric matrix represents the similarity between the community structures at two corresponding time points (Fig. 2*F* illustrates a sample TCS matrix). Specifically, the similarity is evaluated by comparing the node assignments between the two partitions. To quantify this similarity, we use the *z-Rand* score, which assesses the statistical significance of the overlap between communities while accounting for the likelihood of such overlaps occurring by chance. A higher z-Rand score indicates greater similarity between the community structures at the two time points (26).

In addition to the extracted dynamic features, representative average hemodynamic waveforms from auditory and visual ROIs are presented in the *SI Appendix*. These waveforms, along with basic signal characteristics, are included to provide visual context, illustrate region-level response morphology, and support interpretation of task-related activation patterns.

Robustness Analyses. To evaluate the robustness of our approach and address concerns regarding the relative complexity of the spatiotemporal multilayer framework, we conducted supplementary tests. First, we replicated the spatiotemporal model using a simpler spatial framework by applying Louvain community detection independently to each FC window and computing *participation coefficients* to evaluate connectivity within vs. between network communities (57, 58). Second, we assessed the stability of the detected modules by comparing modularity values (Q) from the real networks with those from randomized null models of each window's FC that preserve degree and strength distributions (59). Finally, we examined whether average community size differed across groups (NH, CI1, CI2), since variability in module size could potentially influence switching rates. The results of these robustness checks are presented in the *SI Appendix*.

Data, Materials, and Software Availability. All analysis code, raw data, and supporting materials are publicly available at ref. 60. The repository includes 30 raw recordings from 20 participants (10 CI users with two sessions each, and 10 NH), detected community matrices for all subjects, group-average fNIRS waveforms across all task conditions and groups, the full analysis code (including preprocessing, community detection, feature extraction, and regression modeling), and two illustrative video files. Full access to the raw dataset is subject to approval by the Bionics Institute.

ACKNOWLEDGMENTS. This study was supported by the National Health and Medical Research Council of Australia (GNT1163894 Ideas Grant to C.M.), a Junior Fellowship from the Passe and Williams Foundation (JF_2022_TP to T.P.), and the University of Melbourne Research Scholarship (625441 to J.E.). The Bionics Institute acknowledges the support it receives from the Victorian Government through its Operational Infrastructure Support Program.

Author affiliations: [a]Department of Medical Bionics, University of Melbourne, Parkville, VIC 3052, Australia; [b]Bionics Institute, Fitzroy, VIC 3065, Australia; [c]Department of Electronic, Electrical and Systems Engineering, University of Birmingham, Edgbaston, Birmingham B152TT, United Kingdom; and [d]Department of Speech, Language, and Hearing Sciences, Purdue University, West Lafayette, IN 47907

1. I. Boisvert, M. Reis, A. Au, R. Cowan, R. C. Dowell, Cochlear implantation outcomes in adults: A scoping review. *PLoS One* **15**, e0232421 (2020).
2. P. Blamey *et al.*, Factors affecting auditory performance of postlinguistically deaf adults using cochlear implants: An update with 2251 patients. *Audiol. Neurotol.* **18**, 36–47 (2013).
3. D. S. Lazard *et al.*, Pre-, per-and postoperative factors affecting performance of postlinguistically deaf adults using cochlear implants: A new conceptual model over time. *PLoS One* **7**, e48739 (2012).
4. C. C. Dunn *et al.*, Longitudinal speech perception and language performance in pediatric cochlear implant users: The effect of age at implantation. *Ear Hear.* **35**, 148 (2014).
5. K. A. Buckley, E. A. Tobey, Cross-modal plasticity and speech perception in pre- and postlingually deaf cochlear implant users. *Ear Hear.* **32**, 2–15 (2011).
6. J. Campbell, A. Sharma, Visual cross-modal re-organization in children with cochlear implants. *PLoS One* **11**, e0147793 (2016).
7. G. A. Calvert *et al.*, Activation of auditory cortex during silent lipreading. *Science* **276**, 593–596 (1997).
8. A.-L. Giraud, H.-J. Lee, Predicting cochlear implant outcome from brain organisation in the deaf. *Restor. Neurol. Neurosci.* **25**, 381–390 (2007).
9. D. S. Lee *et al.*, Cross-modal plasticity and cochlear implants. *Nature* **409**, 149–150 (2001).
10. Y.-T. Mao, S. L. Pallas, Cross-modal plasticity results in increased inhibition in primary auditory cortical areas. *Neural Plast.* **2013**, 530651 (2013).
11. K. Strelnikov *et al.*, PET-imaging of brain plasticity after cochlear implantation. *Hear. Res.* **322**, 180–187 (2015).
12. K. Strelnikov *et al.*, Visual activity predicts auditory recovery from deafness after adult cochlear implantation. *Brain* **136**, 3682–3695 (2013).
13. L.-C. Chen, S. Puschmann, S. Debener, Increased cross-modal functional connectivity in cochlear implant users. *Sci. Rep.* **7**, 1–10 (2017).
14. J. Esmaelpoor *et al.*, Resting-state functional connectivity predicts cochlear-implant speech outcomes. *Ear Hear.* **46**, 128–138 (2024).
15. J. Esmaelpoor *et al.*, Cross-modal functional plasticity after cochlear implantation. *Cereb. Cortex* **35**, bhaf084 (2025).
16. A. M. Fullerton *et al.*, Cross-modal functional connectivity supports speech understanding in cochlear implant users. *Cereb. Cortex* **33**, 3350–3371 (2022).
17. D. S. Bassett *et al.*, Dynamic reconfiguration of human brain networks during learning. *Proc. Natl. Acad. Sci. U.S.A.* **108**, 7641–7646 (2011).
18. M. Pedersen, A. Zalesky, A. Omidvarnia, G. D. Jackson, Multilayer network switching rate predicts brain performance. *Proc. Natl. Acad. Sci. U.S.A.* **115**, 13376–13381 (2018).
19. U. Braun *et al.*, Dynamic reconfiguration of frontal brain networks during executive cognition in humans. *Proc. Natl. Acad. Sci. U.S.A.* **112**, 11678–11683 (2015).
20. A. Fornito, A. Zalesky, E. Bullmore, *Fundamentals of Brain Network Analysis* (Academic press, 2016).
21. K. Finc *et al.*, Dynamic reconfiguration of functional brain networks during working memory training. *Nat. Commun.* **11**, 2435 (2020).
22. D. Moreno-Dominguez, A. Anwander, T. R. Knösche, A hierarchical method for whole-brain connectivity-based parcellation. *Hum. Brain Mapp.* **35**, 5000–5025 (2014).
23. W.-L. Chen *et al.*, Functional near-infrared spectroscopy and its clinical application in the field of neuroscience: Advances and future directions. *Front. Neurosci.* **14**, 724 (2020).
24. M. J. Shader, R. Luke, N. Gouailhardou, C. M. McKay, The use of broad vs restricted regions of interest in functional near-infrared spectroscopy for measuring cortical activation to auditory-only and visual-only speech. *Hear. Res.* **406**, 108256 (2021).
25. P. J. Mucha, T. Richardson, K. Macon, M. A. Porter, J.-P. Onnela, Community structure in time-dependent, multiscale, and multiplex networks. *Science* **1979**, 876–878 (2010).
26. V. Red, E. D. Kelsic, P. J. Mucha, M. A. Porter, Comparing community structure to characteristics in online collegiate social networks. *SIAM Rev.* **53**, 526–543 (2011).
27. A. Kral, A. Sharma, Crossmodal plasticity in hearing loss. *Trends Neurosci.* **46**, 377–393 (2023).
28. R. S. Tyler, A. J. Parkinson, G. G. Woodworth, M. W. Lowder, B. J. Gantz, Performance over time of adult patients using the Ineraid or Nucleus cochlear implant. *J. Acoust. Soc. Am.* **102**, 508–522 (1997).
29. C. M. McKay *et al.*, "Connectivity in language areas of the brain in cochlear implant users as revealed by fNIRS" in *Physiology, Psychoacoustics and Cognition in Normal and Impaired Hearing*, D. A. Hall, T. J. Tyler, A. Searchfield, Eds. (Springer, Cham, 2016), pp. 327–335.
30. D. A. Smieja *et al.*, Interhemispheric auditory connectivity requires normal access to sound in both ears during development. *Neuroimage* **208**, 116455 (2020).
31. P. A. Yusuf, P. Hubka, J. Tillein, A. Kral, Induced cortical responses require developmental sensory experience. *Brain* **140**, 3153–3165 (2017).
32. P. A. Yusuf, P. Hubka, J. Tillein, M. Vinck, A. Kral, Deafness weakens interareal couplings in the auditory cortex. *Front. Neurosci.* **14**, 625721 (2021).
33. P. A. Yusuf *et al.*, Deficient recurrent cortical processing in congenital deafness. *Front. Syst. Neurosci.* **16**, 806142 (2022).
34. S. Deng, J. Li, B. T. Thomas Yeo, S. Gu, Control theory illustrates the energy efficiency in the dynamic reconfiguration of functional connectivity. *Commun. Biol.* **5**, 295 (2022).
35. K. J. Friston *et al.*, Statistical parametric maps in functional imaging: A general linear approach. *Hum. Brain Mapp.* **2**, 189–210 (1994).
36. J. Esmaelpoor *et al.*, "Brain functional connectivity networks do not return to resting-state during control trials in block design experiments" in *2023 45th Annual International Conference of the IEEE Engineering in Medicine & Biology Society (EMBC)* (IEEE, Piscataway, NJ, 2023), pp. 1–4.
37. E. G. Ceballos *et al.*, The control costs of human brain dynamics. *Netw. Neurosci.* **9**, 77 (2024).
38. A. Hahn *et al.*, Reconfiguration of functional brain networks and metabolic cost converge during task performance. *Elife* **9**, e52443 (2020).
39. E. Bullmore, O. Sporns, The economy of brain network organization. *Nat. Rev. Neurosci.* **13**, 336–349 (2012).
40. O. Sporns, Graph theory methods: Applications in brain networks. *Dialogues Clin. Neurosci.* **20**, 111–121 (2018).
41. M. Sur, "Rewiring cortex: Cross-modal plasticity and its implications for cortical development and function" in *Handbook of Multisensory Processing*, G. A. Calvert, C. Spence, B. E. Stein, Eds. (MIT Press, 2004), pp. 661–694.
42. S. Steinmann, G. Leicht, C. Mulert, Interhemispheric auditory connectivity: Structure and function related to auditory verbal hallucinations. *Front. Hum. Neurosci.* **8**, 55 (2014).
43. C. Karoui *et al.*, Auditory cortical plasticity after cochlear implantation in asymmetric hearing loss is related to spatial hearing: A PET H215O study. *Cereb. Cortex* **33**, 2229–2244 (2023).

Downloaded from https://www.pnas.org by UNIVERSITY OF BIRMINGHAM on January 16, 2026 from IP address 147.188.245.153.

44. D. S. Lazard, H.-J. Lee, E. Truy, A.-L. Giraud, Bilateral reorganization of posterior temporal cortices in post-lingual deafness and its relation to cochlear implant outcome. *Hum. Brain Mapp.* **34**, 1208–1219 (2013).
45. L. Ashendorf *et al.*, Trail making test errors in normal aging, mild cognitive impairment, and dementia. *Arch. Clin. Neuropsychol.* **23**, 129–137 (2008).
46. T. N. Tombaugh, Trail making test A and B: Normative data stratified by age and education. *Arch. Clin. Neuropsychol.* **19**, 203–214 (2004).
47. G. E. Peterson, I. Lehiste, Revised CNC lists for auditory tests. *J. Speech Hear. Disord.* **27**, 62–70 (1962).
48. P. W. Dawson, A. A. Hersbach, B. A. Swanson, An adaptive Australian sentence test in noise (AuSTIN). *Ear Hear.* **34**, 592–600 (2013).
49. R. L. Sherbecoe, G. A. Studebaker, Supplementary formulas and tables for calculating and interconverting speech recognition scores in transformed arcsine units. *Int. J. Audiol.* **43**, 442–448 (2004).
50. H. Santosa, X. Zhai, F. Fishburn, T. Huppert, The NIRS brain AnalyzIR toolbox. *Algorithms* **11**, 73 (2018).
51. L. Pollonini *et al.*, Auditory cortex activation to natural speech and simulated cochlear implant speech measured with functional near-infrared spectroscopy. *Hear. Res.* **309**, 84–93 (2014).
52. F. A. Fishburn, R. S. Ludlum, C. J. Vaidya, A. V. Medvedev, Temporal derivative distribution repair (TDDR): A motion correction method for fNIRS. *Neuroimage* **184**, 171–179 (2019).
53. L. Kocsis, P. Herman, A. Eke, The modified beer-lambert law revisited. *Phys. Med. Biol.* **51**, N91 (2006).
54. H. Santosa, X. Zhai, F. Fishburn, P. J. Sparto, T. J. Huppert, Quantitative comparison of correction techniques for removing systemic physiological signal in functional near-infrared spectroscopy studies. *Neurophotonics* **7**, 35009 (2020).
55. U. Wolf *et al.*, Correlation of functional and resting state connectivity of cerebral oxy-, deoxy-, and total hemoglobin concentration changes measured by near-infrared spectrophotometry. *J. Biomed. Opt.* **16**, 87013 (2011).
56. M. E. J. Newman, M. Girvan, Finding and evaluating community structure in networks. *Phys. Rev. E* **69**, 26113 (2004).
57. R. Guimera, L. A. N. Amaral, Cartography of complex networks: Modules and universal roles. *J. Stat. Mech. Theory Exp.* **2005**, P02001 (2005).
58. V. D. Blondel, J.-L. Guillaume, R. Lambiotte, E. Lefebvre, Fast unfolding of communities in large networks. *J. Stat. Mech.* **2008**, P10008 (2008).
59. M. Rubinov, O. Sporns, Weight-conserving characterization of complex functional brain networks. *Neuroimage* **56**, 2068–2079 (2011).
60. L. Esmaelpoor, Dynamic functional connectivity following cochlear implantation [data and code repository]. GitHub. https://github.com/jesmaelpoor/Dynamic-Functional-Connectivity-Following-Cochlear-Implantation. Accessed 26 November 2025.

Downloaded from https://www.pnas.org by UNIVERSITY OF BIRMINGHAM on January 16, 2026 from IP address 147.188.245.153.